Asian Journal of Physics Vol. 18, No. 2 (2009) 211-222

A study on the excitation and the input impedance of an antenna

Kuniaki Yoshitomi
Department of Computer Science and Communication Engineering, Kyushu University
744 Motooka, Nishi-ku, Fukuoka 819-0395, Japan

Several source models which can be used in the numerical solution of the electric field integral equation (EFIE) using thin wire theory are studied. These source models include the conventional delta gap source, a magnetic ribbon source, an infinitesimal dipole source, and the magnetic frill source. The magnetic ribbon source model is derived by the equivalent magnetic current corresponding to the gap field. In the thin wire theory it was found that the magnetic ribbon source and an infinitesimal dipole source provide more stable input impedance than the delta gap source or the magnetic frill source.

1 Introduction

To excite thin wire antennas, there are two feeding structures, a gap feeding for dipole antennas, Fig. 1(a), and a coaxial line feeding through a ground plane for monopole antennas, Fig. 2(a). In the thin wire formulation of the method of moments (MoM), there have been two methods used to model these feeding structures [1]. One is the delta gap source modeling as shown in Fig. 1(b), which is the simplest and widely used, however, it was found to yield inaccurate results, especially for impedances. The other source model is the magnetic frill source as shown in Fig. 2(b).

The delta gap source model is one in which a constant longitudinal electric field is applied over a single segment. If the length of segment is reduced as the number of segments is increased, then the source region also gets small. This gives rise to a gap capacitance which causes the numerical results to differ from those actually expected in a physical situation. To eliminate this problem, a delta gap source model containing more than just one segment has been presented [2, 3]. Another source model of this kind is an extended delta gap source model [4]. The electric field of this source model is tapered with the Gaussian function and extends over the dipole.

The magnetic frill source was introduced to calculate the near- as well as the far-zone fields from coaxial aperture [5-7]. In this model, the feed gap is replaced with a circumferentially directed magnetic current density, and the fields generated by the magnetic frill current can be obtained rigorously.

In this paper we will investigate a magnetic ribbon source model as shown in Fig. 1(c), and an infinitesimal dipole source model as shown in Fig. 1(d). These source models can be expressed by simple closed forms and virtually independent of the length of the feed gaps. The fields obtained by these source models are stable and similar to the field provided by the magnetic frill source model. The relation among these models, the magnetic frill source, and the infinitesimal dipole are discussed.

2 Theory

A center-fed dipole antenna is shown in Fig. 1(a). A voltage V is applied across the feed gap of length δ and generates the incident field $\mathbf{E}^i$ over the complete domain of the antenna. Usually the problem is replaced with an equivalent one consisting of a dipole without a gap at its feed point, but with a ribbon of impressed magnetic current at the surface of the gapless dipole at the position of the gap in the original problem as shown in Fig. 1(c).

Corresponding author :
E-mail: yositomi@csce.kyushu-u.ac.jp (Dr Kuniaki Yoshitomi)

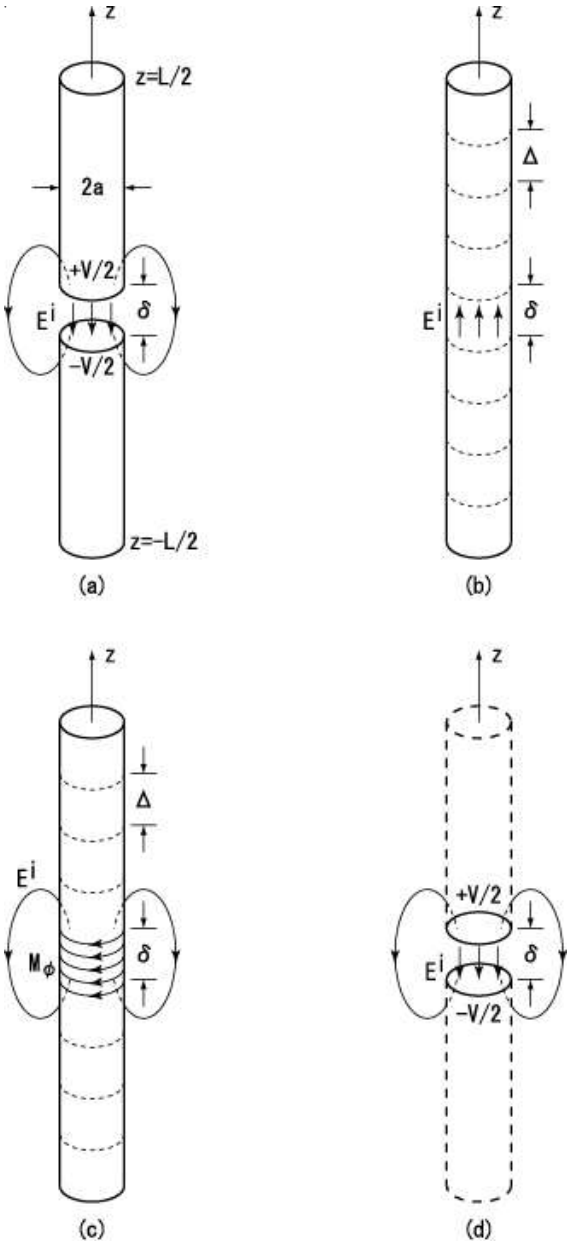

Fig. 1(a). Dipole antenna with impressed voltage V, (b) delta gap source model, (c) magnetic ribbon source model, (d) infinitesimal dipole source model.

2.1 Conventional delta gap model

In the conventional delta gap model, Fig. 1(b), however, the incident field $\mathbf{E}^i = \mathbf{E}^g$ is defined to be nonzero only within a small localized region of the antenna:

$$E_z^g(a, \varphi, z) = \begin{cases} V/\delta, & |z| \le \delta/2, \\ 0, & \text{otherwise.} \end{cases} \tag{1}$$

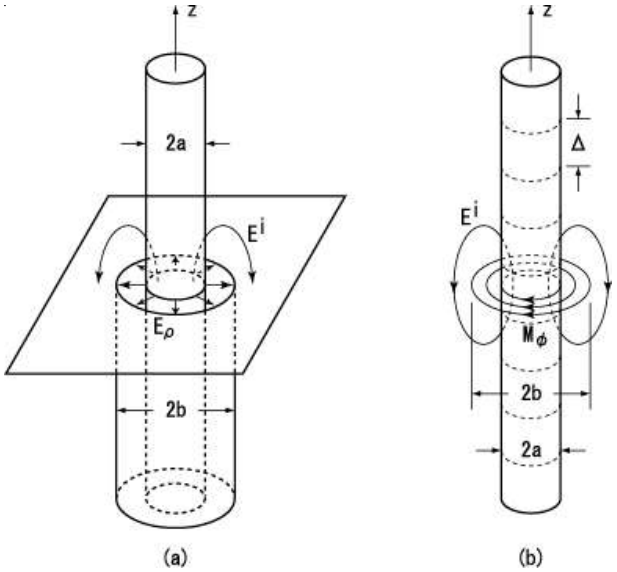

Fig. 2(a). Coaxial line feeding a monopole through a ground plane, (b) magnetic frill source model.

And furthermore, the original gap length δ is replaced with the length of a fictitious gap Δ, which is actually a single element of the segmented gapless antenna and varies with the number of segment. Therefore this is called a variable gap model.

The effect of the gap model which consists of more than one segment was discussed by Tesche [2] and Werner [3]. They concluded that a variable gap model can cause large errors in the method of moment solution, and that a constant gap model improves this problem.

2.2 Magnetic ribbon model

If the magnetic current $\mathbf{M}_r$ is defined by

$$\mathbf{M}_r = \begin{cases} -\hat{\mathbf{a}}_\varphi V/\delta, & |z| \le \delta/2, \\ 0, & \text{otherwise.} \end{cases} \tag{2}$$

we have an incident field $\mathbf{E}^i = \mathbf{E}^r$ which has the same z-component between the gap given in Eq (1). The electric vector potential $\mathbf{F}_r$ associated with the magnetic current $\mathbf{M}_r$ is given by

$$\mathbf{F}_r(\mathbf{r}) = \frac{\varepsilon_0}{4\pi}\iint_{ribbon} \mathbf{M}_r(\mathbf{r}') \frac{\exp(-jk|\mathbf{r}-\mathbf{r}'|)}{|\mathbf{r}-\mathbf{r}'|} ds' \tag{3}$$

Where $\mathbf{r}$ and $\mathbf{r}'$ are the observation point and the source point, respectively. Substituting Eq (2) into Eq (3) we have

$$\mathbf{F}_r(\mathbf{r}) = -\hat{\mathbf{a}}_\varphi \frac{\varepsilon_0 aV}{2\pi\delta} \int_0^{\pi}\int_{-\delta/2}^{\delta/2} \cos\varphi' \frac{\exp(-jkR')}{R'} d\varphi' dz' \tag{4}$$

where $R' = [(z-z')^2 + \rho^2 + a^2 - 2a\rho\cos\varphi']^{1/2}$. The fields $\mathbf{E}^r$, $\mathbf{H}^r$ are given by

$$E_z^r = -\frac{1}{\varepsilon_0}\frac{\partial}{\rho\partial\rho}(\rho F_\varphi^r),\ E_\rho^r = \frac{1}{\varepsilon_0}\frac{\partial}{\partial z}F_\varphi^r,\ H_\varphi^r = -j\omega F_\varphi^r \quad \textit{Author:Correction} \tag{5}$$

where E_φ^r, H_ρ^r and H_z^r are identically zero.

To find the field from the vector potential numerical differentiation is required except for the axial fields which can be obtained in a simple form as follows [5]. On the axis at $\rho = 0$, we have

$R' = [(z - z')^2 + a^2]^{1/2}$, hence

$$F_\varphi^r\ (0, z) = -\frac{\varepsilon_0 a V}{2\pi\delta} \times \int_0^{\pi} \cos\varphi' d\varphi' \int_{-\delta/2}^{\delta/2} \frac{\exp(-jkR')}{R'} dz' \equiv 0 \tag{6}$$

From Eq (5),

$$E_z^r\ (0, z) = \lim_{\rho \to 0} \left[-\frac{1}{\varepsilon_0} \frac{F_\varphi^r}{\rho} - \frac{1}{\varepsilon_0} \frac{\partial F_\varphi^r}{\partial \rho} \right] = -\frac{2}{\varepsilon_0} \frac{\partial F_\varphi^r}{\partial \varphi}\bigg|_{\rho=0} \tag{7}$$

where l'Hospital's rule is used to account for the $0/0$ term.

Substituting Eq (6) into Eq (7) leads to

$$E_z^r\ (0, z) = \frac{aV}{\pi\delta} \times \int_0^{\pi} \int_{-\delta/2}^{\delta/2} \cos\varphi' \left[\frac{\partial}{\partial \rho} \frac{\exp(-jkR')}{R'} \right] d\varphi' dz' \tag{8}$$

Since

$$\frac{\partial R'}{\partial \rho}\bigg|_{\rho = 0} = \frac{\rho - a\cos\varphi'}{R'}\bigg|_{\rho = 0} = -\frac{a\cos\varphi'}{R'} \tag{9}$$

we find

$$E_z^r\ (0, z) = \frac{aV}{2\delta} \times \int_0^{\pi} (-a\cos^2\varphi') d\varphi' \int_{-\delta/2}^{\delta/2} \frac{d}{dR'} \frac{\exp(-jkR')}{R'} dz' = \frac{a^2 V}{2\delta} \int_{-\delta/2}^{\delta/2} \frac{1 + jkR'}{R'^3} \exp(-jkR') dz' \tag{10}$$

In the limit as $\delta \to 0$, magnetic ring source, Eq (10) reduces to

$$E_z^r\ (0, z) = \frac{a^2 V}{2} \frac{1 + jkR_0}{R_0^3} \exp(-jkR_0) \tag{11}$$

with $R_0 = \sqrt{R^2 + a^2}$.

For the magnetic field defined in Eq (2), a constant electric field in the gap is assumed. A much realistic field distribution including feed-point singularity has the form [8]

$$E_z(z) = -\frac{2V}{\pi\sqrt{\delta^2 - 4z^2}}\ . \tag{12}$$

In this case, Eq (4) can be written as follows

$$\mathbf{E}_{r,\,s}\ (\mathbf{r}) = -\hat{\mathbf{a}}_\varphi \frac{\varepsilon_0 a V}{\pi^2} \times \int_0^{\pi} \int_{-\delta/2}^{\delta/2} \frac{\cos\varphi'}{\sqrt{\delta^2 - 4z'^2}} \frac{\exp(-jkR')}{R'} d\varphi' dz' \tag{13}$$

and Eq (10) is also written as

$$E_z^{r,s}(0,z) = \frac{a^2 V}{\pi} \times \int_{-\delta/2}^{\delta/2} \frac{1 + jkR'}{\sqrt{\delta^2 - 4z'^2}\, R'^3} \exp(-jkR') dz' \tag{14}$$

In the case of the limit as $\delta \to 0$, the result is the same as that given Eq (11).

2.4 Infinitesimal dipole model

Let us consider an infinitesimal dipole or a small capacitor-plate antenna shown in Fig. 1 (d). The field $\mathbf{E}^{\mathrm{d}}$ produced by the infinitesimal dipole placed at $x = y = z = 0$ is

$$E_r^d(r,\theta) = \frac{m \cos\theta}{2\pi\varepsilon_0} \frac{(1 + jkr)\exp(-jkr)}{r^3} \tag{15}$$

$$E_\theta^d(r,\theta) = \frac{m \sin\theta}{4\pi\varepsilon_0} \frac{[1 + jkr - (kr)^2]\exp(-jkr)}{r^3} \tag{16}$$

where $E_\varphi^d = 0$ and the electric moment m is given by

$$m = Q\delta \tag{17}$$

where Q is the charge which is determined by the capacitance $C = 2\pi\varepsilon_0 a^2/\delta$ and the applied voltage V, therefore $m = CV\delta = 2\pi\varepsilon_0 a^2 V$. Substituting this into Eqs (15) and (16), we have

$$E_r^d(r,\theta) = \frac{a^2 V \cos\theta}{4} \frac{(1 + jkr)\exp(-jkr)}{r^3} \tag{18}$$

$$E_\theta^d(r,\theta) = \frac{a^2 V \sin\theta}{4} \frac{[1 + jkr - (kr)^2]\exp(-jkr)}{r^3} \tag{19}$$

In the vicinity of the axis, $\rho < |z|$, the axial component of the electric field reduces to

$$E_z^d(\rho,z) = E_r^g \cos\theta - E_0^g \sin\theta \cong \frac{a^2 V}{2} \frac{(1 + jkr)\exp(-jkr)}{r^3} \tag{20}$$

where $r = \sqrt{z^2 + \rho^2}$. Equation (20) is identical to Eq (11) on the surface of the antenna, $\rho = a$, $|z| \le L/2$.

2.3 Magnetic frill model

The incident field $\mathbf{E}'$ produced by a magnetic frill of outer radius b located at the center of the dipole, Fig. 2 (b), is obtained by the electric vector potential $\mathbf{F}_f$ given by

$$\mathbf{F}_f(\mathbf{r}) = -\hat{\mathbf{a}}_\varphi \frac{\varepsilon_0 V}{2\pi \ln(b/a)} \times \int_0^\pi \int_a^b \cos\varphi' \frac{\exp(-jkR')}{R'} d\varphi' d\rho' \tag{21}$$

where $R' = [z^2 + \rho^2 + a^2 - 2a\rho\cos\varphi']^{1/2}$ and the electric field of TEM mode is assumed over the annular aperture of the magnetic frill.

The axial electric field is expressed by the exact closed form as

$$E_z^f(0,z) = \frac{V}{2 \ln(b/a)} \left[\frac{\exp(-jkR_a)}{R_a} - \frac{\exp(-jkR_b)}{R_b} \right] \tag{22}$$

where, $R_a = \sqrt{z^2 + a^2}$, $R_b = \sqrt{z^2 + b^2}$. In the limit $b \to a$, Eq (22) reduces to the same expression as that given in Eq (11). The ratio b/a *is* determined by the characteristic impedance Z_c of the annular aperture, feeding coaxial cable, and usually a 50-ohm characteristic impedance is chosen [1]:

$$Z_c = \sqrt{\frac{\mu_0}{\varepsilon_0}} \frac{l_n(b/a)}{2\pi} = 50, \frac{b}{a} = 2.3 \tag{23}$$

3 Numerical Results

Let us consider a straight cylindrical antenna as shown in Fig. 1(a). The antenna has a total length L, radius a, and is center driven with a gap at $z = 0$. The current $I(z)$ which is an equivalent filament line-

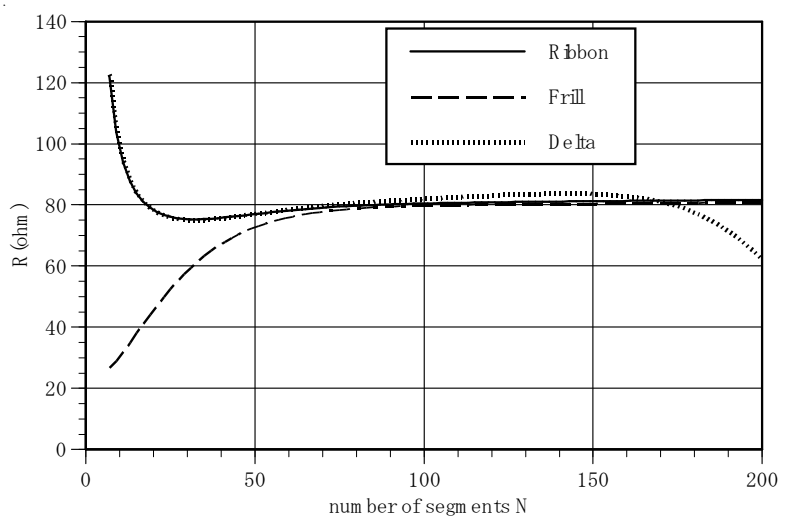

(a) R versus N for a half wave dipole.

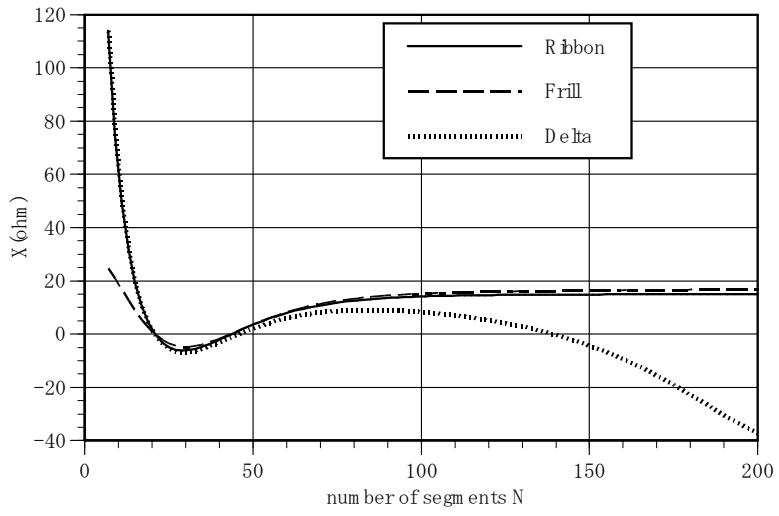

(b) X versus N for a half wave dipole.

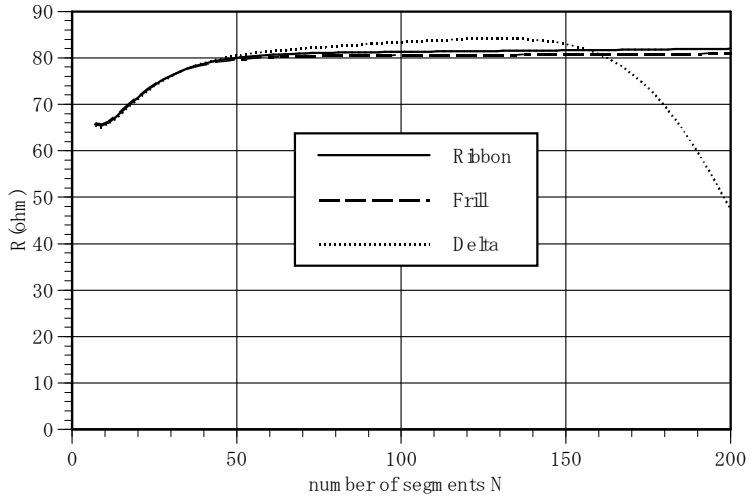

(c) R versus N for a half wave dipole.

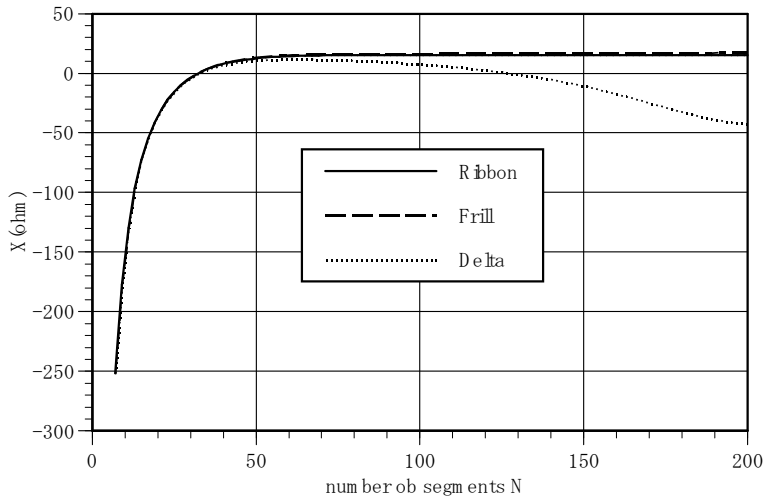

(d) X versus N for a half wave dipole.

Fig. 3. Curves showing convergence of input impedance for three different sources: delta gap, frill, and ribbon. (a) and (b) are solutions of a point matching method, and (c) and (d) are solutions of Galerkin method. For ribbon source, Eq (10) was used in (a) and (b), whereas Eq (11) was used in (c) and (d). $L = 0.47\lambda$, $a = 0.005\lambda$.

source current located a radial distance $\rho = a$ from z axis satisfies the Pocklington's integral equation:

$$\frac{-1}{j\omega\varepsilon_0}\int_{-L/2}^{L/2} I(z')\left(\frac{d^2}{dz^2}+k^2\right)\times\frac{\exp\left[-jk\sqrt{(z-z')^2+a^2}\right]}{\sqrt{(z-z')^2+a^2}}\,dz' = E_z^i(z) \tag{24}$$

In solving this equation by the method of moments, we used the pulse functions. The weighting functions used were impulses (a point matching method), or pulse functions (Galerkin method).

Fig. 3(a)-(d) shows the convergence of input impedance for three different source models: the delta gap, the frill, and the ribbon. The infinitesimal dipole source has the same property as that of the

ribbon source. For the delta gap source (1), and the ribbon source (10), the gap width $\delta = \Delta = L/N$, where Δ is the segment length and is the number of segments. Therefore both the delta gap model and the ribbon model are the variable gap model, the input impedance of the delta gap model diverges for large N. However the input impedance of the ribbon model converges to a stable result. This is because the incident field produced by the magnetic ribbon source is virtually independent of the gap width.

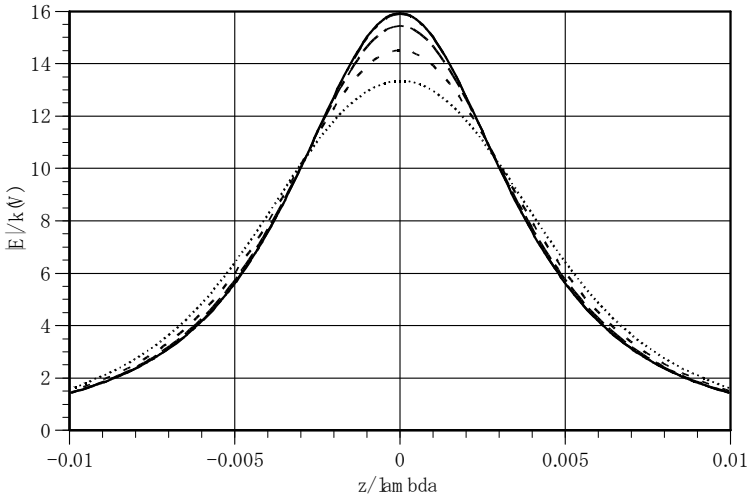

(a) $\left|E_z^r\right|/k$ versus z/λ

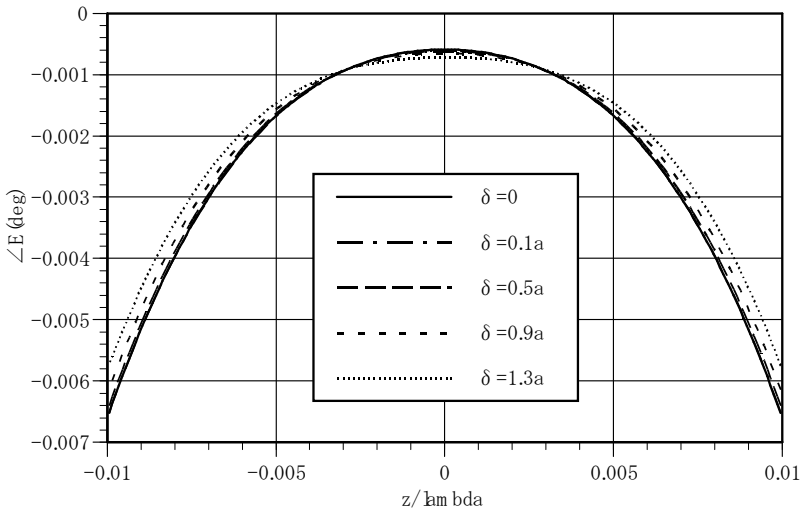

(b) $\angle E_z^r$ versus z/λ

Fig. 4. Incident electric field on the axis excited by the magnetic ribbon source given by (10) for different gap length δ where $a = 0.005\lambda$.

Figure 4(a)-(b) show the incident electric fields on the axis excited by the magnetic ribbon source. The incident fields of the magnetic frill are shown in Fig. 5(a)-(b) for different ratio b/a. It is found that both amplitude and phase change strongly depending on the ratio b/a. The incident fields of the ribbon model including feed-point singularity (Fig. 6) are similar to those of the constant field magnetic ribbon.

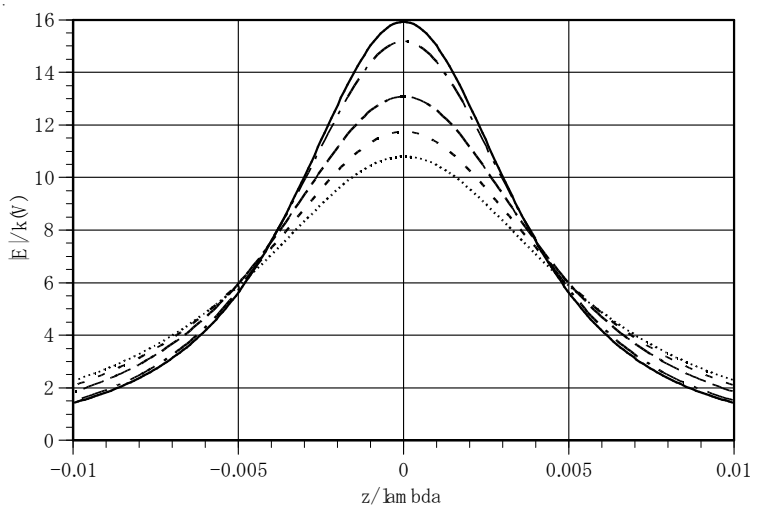

(a) $\left|E_z^f\right|/k$ versus z/λ

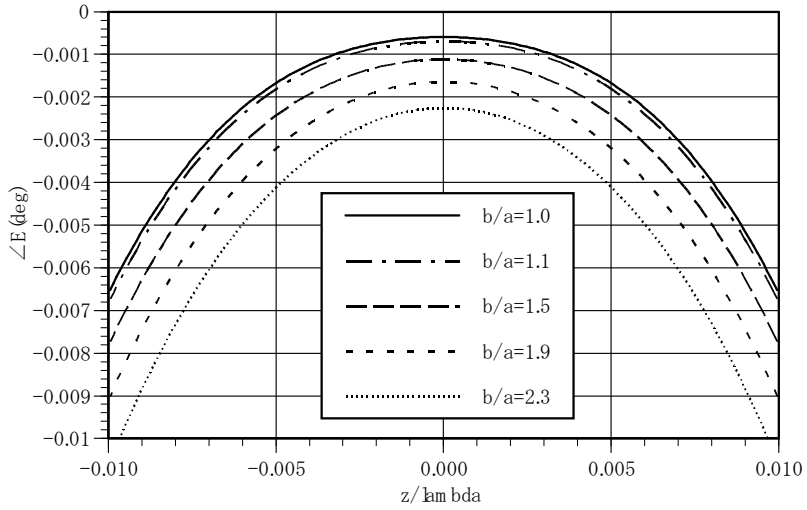

(b) $\angle E_z^f$ versus z/λ

Fig. 5. Incident electric field on the axis excited by the magnetic frill source given by Eq (22) for different ratios b/a, where $a = 0.005\lambda$.

The input impedance of a thin dipole antenna of radius $a = 7.022 \times 10^{-1}\ \lambda$ is shown in Fig. 7(a)-(b) [9]. The impedances of the magnetic ribbon model and the frill model agree well in a wide rage of frequency. However, both impedances will not agree completely even if the calculation is accurately done, because the incident field distributions produced by those source models are different. This difficulty might be resolved if the source model in which the length of the feed gap is zero such as the ribbon source given in Eq (11), the infinitesimal dipole source given in Eq (20), and the frill source with the ratio $b/a = 1$. These sources are magnetic ring current sources or equivalent electric dipoles.

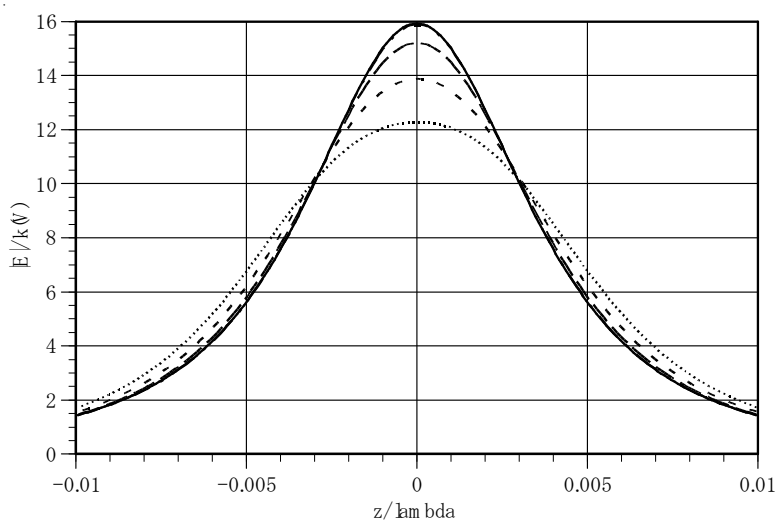

(a) $\left|E_z^r\right|/k$ versus z/λ

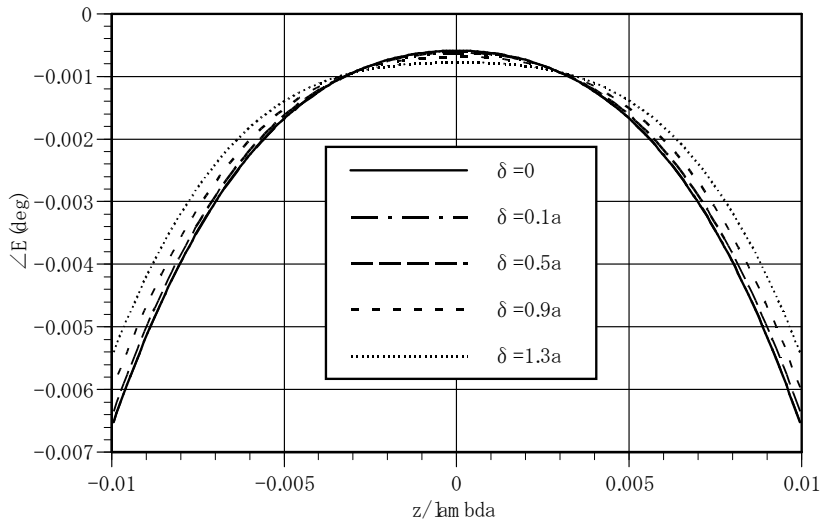

(b) $\angle E_z^r$ versus z/λ

Fig. 6. Incident electric field on the axis excited by the magnetic ribbon source given by Eq (14) for different gap length δ where $a = 0.005\lambda$.

4 Conclusion

The input impedance of an antenna is defined as the impedance presented by the antenna at its terminals [9]. In this paper it was found that the calculated input impedance of a dipole antenna varies with

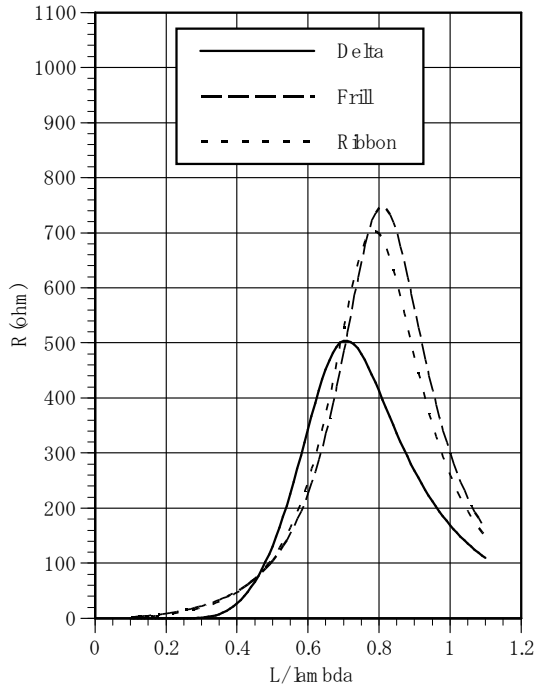

(a) R versus L/λ.

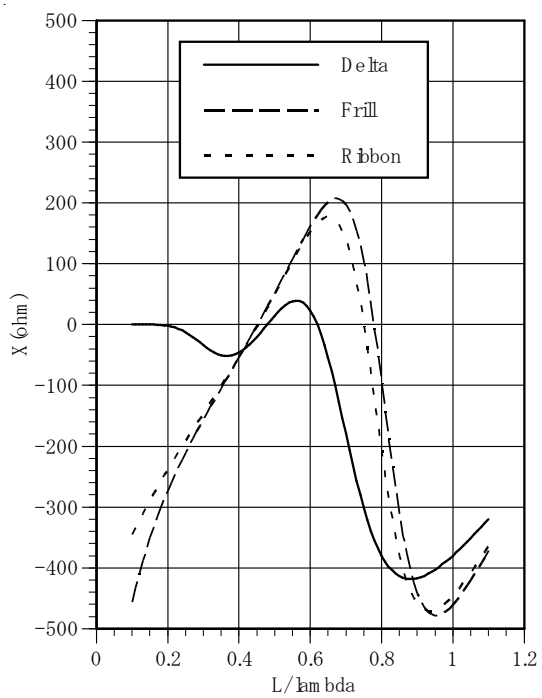

(b) X versus L/λ.

Fig. 7. Input impedance of a thin dipole antenna of radius $a = 7.022 \times 10^{-3}\,\lambda$. Point matching method was used with $N = 101$. In the frill model $b/a = 2.3$ is assumed.

the source models used. One way to eliminate this problem is to use a magnetic ring current source model or an equivalent infinitesimal dipole source model.

References

1. Balanis CA, *Antenna Theory*, (John Wiley & Sons, New York), 1997.
2. FM Tesche,The Effect of the Thin-Wire Approximation and the Source Gap Model on the High-Frequency Integral Equation Solution of Radiating Antennas, *IEEE Trans Antennas Propagat*, 20(1972)210-211.
3. Werner DH, A Method of Moments Approach for the Efficient and Accurate Modeling of Moderately Thick Cylindrical Wire Antennas, *IEEE Trans Antennas Propagat*, 46(1998)373-382.
4. Junker GP, Kishk AA, Glisson AW, A Novel Delta Gap Source Model for Center Fed Cylindrical Dipoles, *IEEE Trans Antennas Propagat*, 43(1995)537-540.
5. Tsai LL, A Numerical Solution for the Near and Far Fields of an Annular Ring of Magnetic Current, *IEEE Trans Antennas Propagat*, 20(1972)569-576.
6. Peterson AF, Bibby MM, High-Order Numerical Solutions of the MFIE for the Linear Dipole, *IEEE Trans Antennas Propagat*, 52 (2004)2684-2691.
7. Heldring A, Ubeda E, Rius JM, Efficient Computation of the Effect of Wire Ends in Thin Wire Analysis, *IEEE Trans Antennas Propagat*, 54(2006)3034-3037.
8. Hurd RA, Jacobsen J, Admittance of an Infinite Cylindrical Antenna with Realistic Gap Field, *Electronics Letters*, 4(1968)420-421.
9. Stutzman WL,Thiele GA, Antenna Theory and Design, (John Wiley & Sons,New York), 1998.

[*Received* : 27.3.09; *accepted* : 30.5.09]